

Influence of Roof Slope on Timber Consumption in Plane Trusses Design

Iuri Fazolin Fraga,^a Matheus Henrique Morato de Moraes,^a Isabella Silva Menezes,^a Felipe Nascimento Arroyo,^{a,*} João Paulo Boff de Almeida,^a Edson Fernando Castanheira Rodrigues,^a Fernando Resende Mascarenhas,^a Vinícius Borges de Moura Aquino,^b Sérgio Augusto Mello Silva,^c Francisco Antonio Rocco Lahr,^d Wanderlei Malaquias Pereira Júnior,^e and André Luis Christoforo^a

The growing world consumption of wood in civil construction is evident, especially in structural roofing systems. Despite being from a renewable source, its rational and intelligent use is of vital importance in the execution of structural designs. Because it is a system that is recognized worldwide in the design of trussing roof structures, there are several empirical assumptions for structural calculation. To reduce timber consumption, some tile manufacturers suggest a 10% (6°) slope between chords. However, after simulations of 11 slopes with angles from 5° to 15°, the timber consumption was inversely proportional to the slope, reaching a 90% difference between extreme angles. The method used to obtain the results was software designed according to the routines prescribed by the new draft standard of ABNT NBR 7190 (2021). Considering a prefabricated truss with 5 cm thickness sections, the design criterion was that of minimum height, increasing by 0.10 cm until all checks were satisfied. Finally, the minimum angle after which no strengthening is required on the bars was 10°.

Keywords: Timber structures; Plane trusses; Slope; Design; Timber consumption

Contact information: a: Department of Civil Engineering (DECiv), Federal University of Sao Carlos, Sao Carlos; b: Department of Civil Engineering, Federal University of the South and Southeast of Para, Santana do Araguaia, Brazil; c: Department of Civil Engineering, Paulista State University Júlio de Mesquita Filho, Ilha Solteira, Brazil; d: Wood and Timber Structures Laboratory, Department of Structural Engineering, Sao Carlos School of Engineering of Sao Carlos, University of Sao Paulo (USP), Sao Carlos/SP, Brazil; e: Department of Civil Engineering, Goias Federal University, Catalão, Brazil; *Corresponding author: lipe.arroyo@gmail.com

INTRODUCTION

Wood, a renewable material with remarkable mechanical properties, is an excellent alternative for structural systems (de Almeida *et al.* 2017). Due to its advantages, it is widely used in buildings around the world, especially in single-family homes in countries in the Northern Hemisphere (Wherry and Buehlmann 2014; De Araujo *et al.* 2016).

In Brazil, despite some prejudices arising from misinformation about its excellent performance, there has been an increased consumption in structural systems in recent years (Calil Jr *et al.* 2019). Roofing structures are its most evident application, especially in the form of flat lattice systems. In addition, the country is involved in historic roof structure recovery and migration from artisanal construction to the prefabrication process: trusses with bars connected through gang nail plates (GNP) (Guo *et al.* 2013; Isupov and Chaganov 2019), glued laminated timber structures (Glulam) (Lestari *et al.* 2015; Li *et al.* 2018; Dias

et al. 2020), and cross laminated timber structures (CLT) (Buck *et al.* 2016; Brandt *et al.* 2019; Dolan *et al.* 2019).

Wooden structures in roofing systems are frequently investigated. There are countless variables studied: stability, buckling lengths, and bracing of flat trusses (Burdzik and Skorpen 2014; Sejkot *et al.* 2019); structural behavior in the face of stresses arising from the wind action (Stevenson *et al.* 2019; Navaratnam *et al.* 2020); rigidity and behavior of connections in flat wooden trusses (Tenorio *et al.* 2018; Rivera-Tenorio and Moya 2019); and structural and cost optimization in mechanical connections of flat wooden trusses (Olsson 2010; Villar *et al.* 2016; Villar-Garcia *et al.* 2019).

Even in the face of such themes, new variables can be introduced. As it is a system that is renowned worldwide among designers and builders, when designing roofing structures, some empirical assumptions are gaining ground. For example, some fiber cement tile manufacturers recommend the use of a 10% (6°) slope between flanges, justifying the optimization of the wood volume due to the reduction in the lengths of the bars (Oliveira *et al.* 2019). However, this type of configuration can result in significant stresses on the elements, requiring parts with high cross-sectional areas and, consequently, an increase in the volume of wood.

Even though it comes from a renewable source, the unrestrained use of wood generates a large amount of waste from its processing (Eshun *et al.* 2012; Top *et al.* 2018). Thus, the search for less material consumption can have a positive and significant impact, minimizing the environmental impacts caused by wood waste discarded without due control and criteria.

This study evaluated the roof slope influence on wood consumption in flat roof trusses, considering the new NBR 7190 standard project (ABNT 2021) that introduced new approaches regarding the design of structural parts. For this, the iTruss software was developed and validated by Fraga (2020), where it was possible to design 11 trusses with slopes between flanges ranging from 5° (9%) to 15° (27%).

METHODOLOGY

Geometry

Through technical catalogs of corrugated fiber cement tiles (commonly used in industrial/rural buildings), the roof geometry was defined. Starting from the minimum inclination of 9% (5°), the angles varied by 1° to the inclination of 27% (15°), for a total of 11 geometries. Assuming tiles with a thickness of 6 mm and a complementary piece of ridge with a 300 mm flap, the arrangement of 4 tiles of 153 cm (Fig. 1) was sufficient to guarantee the balance stipulated by the catalogs (greater than 25 cm and less than 40 cm). In addition, minimum coverings were specified between tiles per slope range. Thus, for angles greater than or equal to 9% (5°) and less than or equal to 18% (10°), a covering of 25 cm was adopted, and for angles greater than 18% (10°) and smaller or equal to 27% (15°), a covering equal to 23 cm was considered. In view of these considerations, Fig. 1 illustrates the final structural arrangement. Figure 1 shows that, in addition to being similar to the project reality, the truss's areas of influence vary as little as possible with each other, allowing reliable comparisons in the dimensioning and wood consumption for each slope.

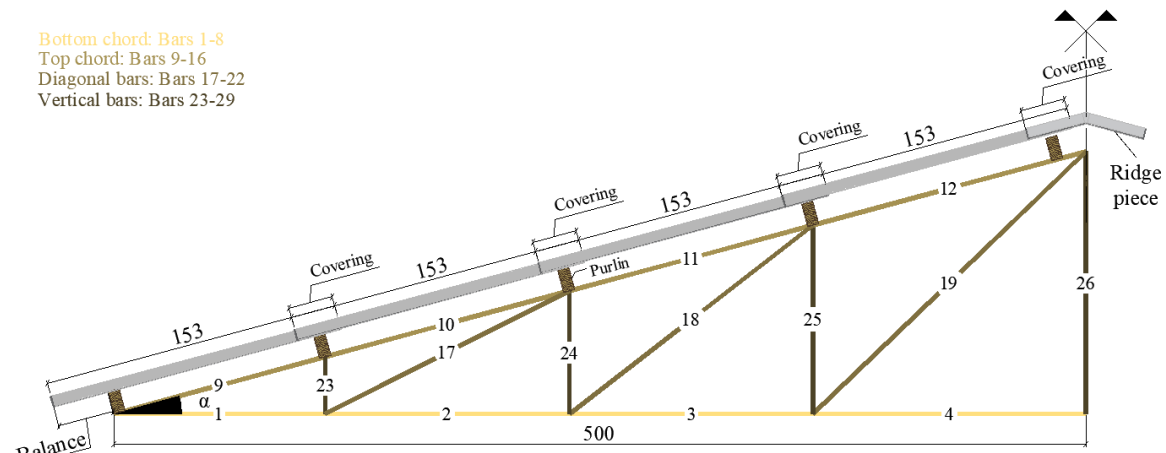


Fig. 1. Bar configuration (dimensions in centimeters)

Loads and Combinations

In roofing projects on wooden structures, the permanent actions come from the structure weight and the roofing materials. The loading due to its own weight does not need to be inserted in the iTruss software, since it adapts minimum sections for each group of bars, automatically updating the structure's weight at each iteration. The variable actions active in this type of project are the overloads in the roof and the wind action. The first ones were estimated according to item 6.4 of ABNT NBR 6120 (2019) and the wind action according to recommendations of the corrected version of ABNT NBR 6123 (2013). The final values adopted are contained in Table 1, as well as the coefficients and factors of combinations of actions adopted for the possible limit states, following the recommendations of the revised ABNT NBR 8681 (2003) and ABNT NBR 7190 (2021).

Table 1. Loads and Combination Coefficients

| Loads | Values (kN/m ²) * | Combination coefficients |
|------------|-------------------------------|--|
| Permanents | 0.25 | $\gamma_g = 1.40$ (unfavorable); $\gamma_g = 1.0$ (favorable) |
| Overload | 0.25 | $\gamma_q = 1.50$; $\psi_0 = 0.7$; $\psi_1 = 0.6$; $\psi_2 = 0.4$ |
| Wind 1 | -1.01 (Left); -1.01 (Right) | $\gamma_q = 1.40$; $\psi_0 = 0.6$; $\psi_1 = 0.3$; $\psi_2 = 0.0$ |
| Wind 2 | -1.21 (Left); -0.68 (Right) | |
| Wind 3 | -0.20 (Left); 0.07 (Right) | |

* Negative values indicate counter-gravity loads

Structural Analysis Model

The calculation model contemplated in this research corresponds to a classic truss, that is, bar elements restricted to axial forces, with perfectly free rotations at their ends. The action due to their own weight was unloaded at the load application points (knots where there are purlins), according to Eq. 1.

$$P = \gamma_{purlin} \cdot A_{purlin} \cdot \frac{l_{purlin}}{2} + \gamma_{roof} \cdot A_{inf} \cdot \frac{l_{purlin}}{2} \quad (1)$$

where P is the concentrated force in the truss; γ_{purlin} the purlin specific weight; A_{purlin} the purlin cross-sectional area; l_{purlin} the purlin length; γ_{roof} the roof (tiles) specific weight; and A_{inf} the roof influence area. Regarding the boundary conditions, the classic isostatic model prevails, that is, a simply supported truss linked in its extreme lower nodes.

Sections and Design

The wood species adopted was the Hardwoods group, class D40. Its characteristic strength values (f), stiffness (E), and apparent specific mass (ρ) were extracted from the standard design of ABNT NBR 7190 (2021), considering parts with moisture content equal to 12%. For the modification coefficients (k_{mod}) estimation, long-term loading class and sawn wood exposed to an environment of relative humidity below 65% [class (1)] were accepted. Therefore, in these conditions, $k_{\text{mod}} = 0.70$.

The purlin was previously dimensioned so that their real forces were applied to the truss together with their own weight. These elements were treated as simply supported beams, whose theoretical span is equal to the distance between trusses, limited here to 3 m. After processing, it was found that the typical 6×12 cm section meets all checks, with a weight of 0.21 kN applied to nodes. However, it is noteworthy that there are two purlins in the ridge knot, assuming, in this place, the value of 0.42 kN.

The criterion used in the dimensioning process was the minimum profile height (h) with thickness fixation (t). The draft standard of ABNT NBR 7190 (2021) recommends that for isolated main parts, the minimum thickness (t) should be 5 cm and the area (A) of the minimum section equal to 50 cm^2 . Thus, starting from this section (5×10 cm) with a fixed thickness ($t = 5$ cm), the smallest height (h) whose area (A) met all the verification criteria was estimated, as observed in the flowchart of Fig. 2.

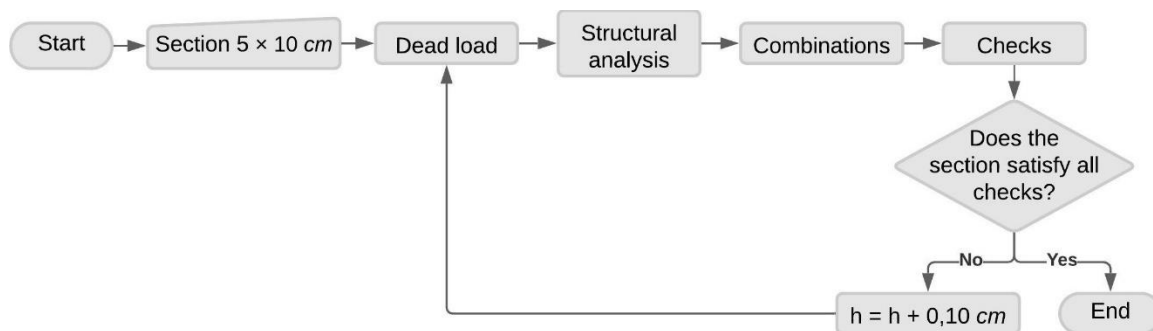


Fig. 2. Routine of the minimum section height criterion

RESULTS AND DISCUSSION

Once the structure has been processed, the wood consumptions expressed in m^3/m^2 , only for truss, each angle analyzed are contained in Fig. 3. The area considered is the result of the product between the span (10 m) and the distance between trusses (3 m), considering the construction of a rectangular plan with regularly spaced porches.

Parallel to the wood consumption calculation, the percentage difference was determined in relation to the smaller volume of material (angle of 15°). These percentage differences are shown in Fig. 4.

When dimensioning each slope, the diagonal bars and uprights do not change, with the minimum section of 5×10 cm prevailing. However, the significant percentage difference in consumption comes from the pieces that make up the flange. It is important to point out that, for an angle of 5° and thinking in a practical point of view, bar 23 in Fig. 1 would have problems of execution near support, since this bar has only 11 cm length, the top and bottom chords will overlap and there will not be enough space in the first panel.

As this angle did not bring positive results, it was kept just to show that the smaller the angle, the greater the wood consumption.

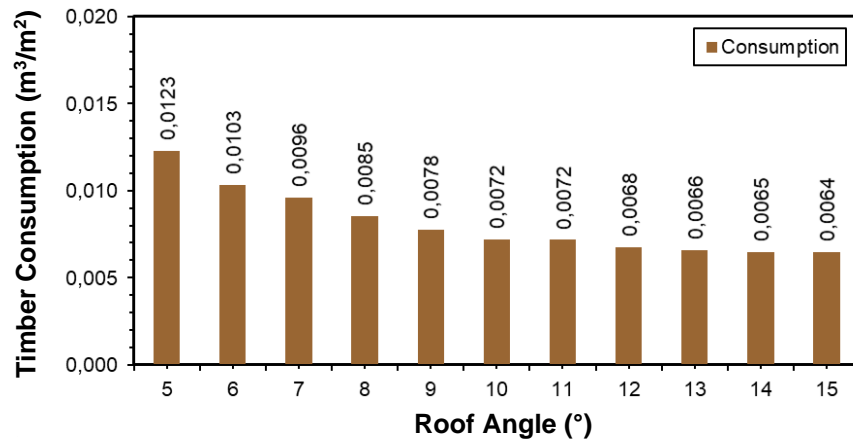


Fig. 3. Roof angle *versus* timber consumption only from the truss

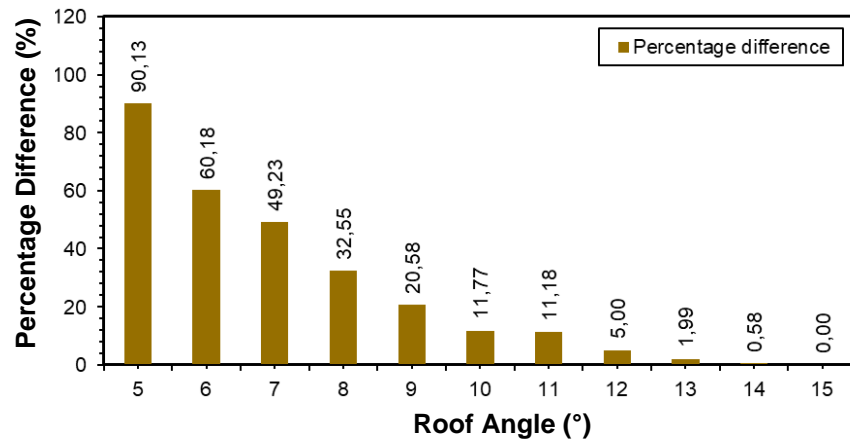


Fig. 4. Percentage differences in relation to the lower volume of timber [angle of 15° (27%)]

In all simulations, the decisive factor in the design was the stability verification due to compression in relation to the axis of least inertia, defined here by the y component. For this situation, the relationship between the design value of the compressive stress acting ($\sigma_{Nc,d}$), and the stability resistance component ($k_{cy} \cdot f_{c0,d}$) configured values very close to or equal to 1. Because the change in the length of the flange at each slope is very small, it is pointed out that the stresses that require compression are responsible for generating exaggerated dimensions as the slope is reduced.

Despite the diagonal bars and uprights reducing their length on smaller slopes, they continue to absorb a small portion of the stresses, significantly increasing the forces on the flange bars that compete for the supports. In other words, it is not due to the simple fact of reducing the length of the diagonal bars and uprights that oversized profiles are observed, but because of the extreme trigonometric reasons, given exclusively by the low angle.

Finally, it remains to be determined what is the minimum slope for which no reinforcement is required on the flange bars. Referring to a table of standardized dimensions of sawn wood, for a thickness (t) of 5 cm, the highest plausible height (h) would be 20 cm. For heights (h) above 20 cm, it is recommended to reinforce the bars through

“T” sections, increase in thickness (t), or even sections composed with parts solidly discontinued with several spacers in order to reduce the buckling length of the elements. However, these measures make material consumption higher. Subsequently, the simulation of all slopes showed that the angle of 10° (18%) corresponds to the minimum capable of generating profiles with heights (h) below 20 cm, producing pieces on the flanges with maximum height (h) equal to 18.8 cm.

CONCLUSIONS

1. The comparisons between the consumption generated by each slope are plausible, given that the values of influence areas are very close to each other.
2. The diagonal bars and uprights profiles do not change during the simulations, with a minimum section of 5×10 cm prevailing. However, the dimensions of the parts that make up the flanges are excessively larger at low slopes.
3. The verification of stability in relation to the axis of least inertia (y) due to centered compression is the factor that drives the profile's design. Since the variation in the flange length is negligible with each inclination, it is concluded that the axial compression stresses, especially in the bars that compete with the supports, are the most responsible for generating such divergent consumption.
4. For the typology and described above, the angle of 10° (18%) is equivalent to the minimum from which reinforcements are not required on the bars, given that the profiles that make up the flanges have heights (h) very close to the maximum dimension here standardized at 20 cm, admitting a fixed thickness (t) of 5 cm.

REFERENCES CITED

- ABNT NBR 6120 (2019). “Ações para o cálculo de estruturas de edificações [Loads for the calculation of building structures],” Associação Brasileira de Normas Técnicas, Rio de Janeiro, Brazil.
- ABNT NBR 6123 (2013). “Forças devidas ao vento em edificações [Wind forces in buildings],” Associação Brasileira de Normas Técnicas, Rio de Janeiro, Brazil.
- ABNT NBR 7190 (2021). “Projeto de estruturas de madeira [Design of timber structures],” Associação Brasileira de Normas Técnicas, Rio de Janeiro, Brazil.
- ABNT NBR 8681 (2003). “Ações e segurança nas estruturas - procedimento [Actions and safety of structures - Procedure],” Associação Brasileira de Normas Técnicas, Rio de Janeiro, Brazil.
- de Almeida, T. H., de Almeida, D. H., De Araujo, V. A., da Silva, S. A. M., Christoforo, A. L., and Lahr, F. A. R. (2017). “Density as estimator of dimensional stability quantities of Brazilian tropical woods,” *BioResources* 12(3), 6579-6590. DOI: 10.15376/biores.12.3.6579-6590
- Brandt, K., Wilson, A., Bender, D., Dolan, J. D., and Wolcott, M. P. (2019). “Techno-economic analysis for manufacturing cross-laminated timber,” *BioResources* 14(4), 7790-7804. DOI: 10.15376/biores.14.4.7790-7804
- Buck, D., Wang, X., Hagman, O., and Gustafsson, A. (2016). “Bending properties of

- cross laminated timber (CLT) with a 45° alternating layer configuration,” *BioResources* 11(2), 4633-4644. DOI: 10.15376/biores.11.2.4633-4644
- Burdzik, W. M. G. and Skorpén, S. A. (2014). “Metal-strip bracing versus diagonal timber bracing in timber trussed tiled roofs,” *Engineering Structures* 75, 1-10. DOI: 10.1016/j.engstruct.2014.05.038
- Calil, C., Jr., Lahr, F. A. R., Martins, G. C. A., and Dias, A. A. (2019). *Estruturas de madeira: Projetos, dimensionamento e exemplos de cálculo [Timber structures: Designs and calculation examples]*, Elsevier, Rio de Janeiro, Brazil.
- De Araujo, V. A., Cortez-Barbosa, J., Gava, M., Garcia, J. N., de Souza, A. J. D., Savi, A. F., Morales, E. A. M., Molina, J. C., Vasconcelos, J. S., Christoforo, A. L., and Lahr, F. A. R. (2016). “Classification of wooden housing building systems,” *BioResources* 11(3), 7889-7901. DOI: 10.15376/biores.11.3.DeAraujo
- Dias, A. M., Martins, C. E. J., and Dias, A. M. P. G. (2020). “Influence of the treatment phase on the gluing performance of glued laminated timber,” *BioResources* 15(3), 5725-5736. DOI: 10.15376/biores.15.3.5725-5736
- Dolan, J. D., Wilson, A., Brandt, K., Bender, D. A., and Wolcott, M. P. (2019). “Structural design process for estimating cross-laminated timber use factors for buildings,” *BioResources* 14(3), 7247-7265. DOI: 10.15376/biores.14.3.7247-7265.
- Eshun, J. F., Potting, J., and Leemans, R. (2012). “Wood waste minimization in the timber sector of Ghana: A systems approach to reduce environmental impact,” *Journal of Cleaner Production* 26, 67-78. DOI: 10.1016/j.jclepro.2011.12.025
- Fraga, I. F. (2020). *Influência dos modelos idealizados de ligações no dimensionamento de treliças planas de madeira [Idealized joints models influence on the design of plane timber trusses]*, Master’s Dissertation, Federal University of São Carlos, São Carlos, Brazil.
- Guo, W., Song, S., Zhao, R., Ren, H., Jiang, Z., Wang, G., Sun, Z., Wang, X., Yang, F., Chen, H., Shi, S. Q., and Fei, B. (2013). “Tension performance of metal-plate connected joints of Chinese larch dimension lumber,” *BioResources* 8(4), 5666-5677. DOI: 10.15376/biores.8.4.5666-5677
- Isupov, S. A. and Chaganov, A. B. (2019). “Strength and stiffness of wood structures for compounds of gang nail plate ‘Steelcap’,” *IOP Conference Series: Materials Science and Engineering* 687, 033015. DOI: 10.1088/1757-899X/687/3/033015
- Lestari, A. S. R. D., Hadi, Y. S., Hermawan, D., and Santoso, A. (2015). “Glulam properties of fast-growing species using mahogany tannin adhesive,” *BioResources* 10(4), 7419-7433. DOI: 10.15376/biores.10.4.7419-7433
- Li, R., Cao, P., Xu, W., Ekevad, M., and Wang, X. (2018). “Experimental and numerical study of moisture-induced stress formation in hexagonal glulam using x-ray computed tomography and finite-element analysis,” *BioResources* 13(4), 7395-7403. DOI: 10.15376/biores.13.4.7395-7403
- Navaratnam, S., Ginger, J., Humphreys, M., Henderson, D., Wang, C.-H., Nguyen, K. T. Q., and Mendis, P. (2020). “Comparison of wind uplift load sharing for Australian truss- and pitch-framed roof structures,” *Journal of Wind Engineering and Industrial Aerodynamics* 204, 104246. DOI: 10.1016/j.jweia.2020.104246
- Oliveira, G. O. B., Pinheiro, R. V., Arroyo, F. N., de Almeida, D. H., de Almeida, T. H., Silva, D. A. L., Christoforo, A. L., Lahr, F. A. R. (2019). “Technical feasibility study of the use of softwoods in lattice structure ‘howe’ type for roofing (gaps between 8-18 meters),” *Current Journal of Applied Science and Technology* 35(4), 1-8. DOI: 10.9734/cjast/2019/v35i430188

- Olsson, A. (2010). "Probabilistic analysis and optimization of roof trusses," *Electronic Journal of Structural Engineering* 10, 74-89.
- Rivera-Tenorio, M. and Moya, R. (2019). "Stress, displacement joints of *Gmelina arborea* and *Tectona grandis* wood with metal plates, screws and nails for use in timber truss connections," *CERNE* 25(2), 172-183. DOI: 10.1590/01047760201925022641
- Sejkot, P., Ormarsson, S., Vessby, J., and Källsner, B. (2019). "Numerical out-of-plane stability analysis of long span timber trusses with focus on buckling length calculations," *Engineering Structures* 204, 109670. DOI: 10.1016/j.engstruct.2019.109670
- Stevenson, S. A., El Ansary, A. M., and Kopp, G. A. (2019). "A practical modelling technique to assess the performance of wood-frame roofs under extreme wind loads," *Engineering Structures* 191, 640-648. DOI: 10.1016/j.engstruct.2019.04.058
- Tenorio, C., Moya, R., Carranza, M., Navarro, A., Saenz, M., and Paniagua, V. (2018). "Mechanical performance in flexure for two spans of trusses from *Hieronyma alchorneoides* and *Gmelina arborea* woods fastened with nails and screws," *Journal of Tropical Forest Science* 30(3), 330-341. DOI: 10.26525/jtfs2018.30.3.330341
- Top, Y., Adanur, H., and Oz, M. (2018). "Type, quantity, and re-use of residues in the forest products industry in Trabzon, Turkey," *BioResources* 13(1), 1745-1760. DOI: 10.15376/biores.13.1.1745-1760
- Villar, J. R., Vidal, P., Fernández, M. S., and Guaita, M. (2016). "Genetic algorithm optimization of heavy timber trusses with dowel joints according to Eurocode 5," *Biosystems Engineering* 144, 115-132. DOI: 10.1016/j.biosystemseng.2016.02.011
- Villar-García, J. R., Vidal-López, P., Rodríguez-Robles, D., and Guaita, M. (2019). "Cost optimization of glued laminated timber roof structures using genetic algorithms," *Biosystems Engineering* 187, 258-277. DOI: 10.1016/j.biosystemseng.2019.09.008
- Wherry, G., and Buehlmann, U. (2014). "Product life cycle of the manufactured home industry," *BioResources* 9(4), 6652-6668. DOI: 10.15376/biores.9.4.6652-6668

Article submitted: May 11, 2021; Peer review completed: August 10, 2021; Revised version received and accepted: August 12, 2021; Published: August 13, 2021.
DOI: 10.15376/biores.16.4.6750-6757